



Synthesis, solvatochromaticity and bioactivities of some transition metal complexes with 2-(R-benzylideneamino)-pyridin-3-ol Schiff base derivatives

I.S. Ahmed*, M.A. Kassem

Chemistry Department, Faculty of Science, Benha University, Benha, Egypt

ARTICLE INFO

Article history:

Received 28 December 2009

Received in revised form 10 March 2010

Accepted 16 March 2010

Keywords:

Schiff base compounds

Elemental analysis

Electronic absorption spectra

Biological activity

ABSTRACT

New four Schiff bases are prepared by condensation of 2-amino-pyridin-3-ol with 3, 4-dihydroxy-benzaldehyde (I), 2-hydroxybenzaldehyde (II), 5-bromo-2-hydroxybenzaldehyde (III), and 4-dimethylaminobenzaldehyde (IV). The structures of these compounds are characterized based on elemental analyses (C, H, N), IR and ^1H NMR. Also, the electronic absorption spectra are recorded in organic solvents of different polarity. The solvents are selected to be covered a wide range of parameters (refractive index, dielectric constant and hydrogen bonding capacity). The UV–vis absorption spectra of Schiff base compounds are investigated in aqueous buffer solutions of varying pH and utilized for the determination of ionization constant, pK_a and activation free energy, ΔG^\ddagger of the ionization process. The biological activity against bacterial species and fungi as microorganisms representing different microbial categories such as (two Gram-negative bacteria, *Escherichia coli* and *Agrobacterium* sp.), three Gram-positive bacteria (*Staphylococcus aureus*, *Bacillus subtilis* and *Bacillus megatherium*), yeast (*Candida albicans*), and fungi (*Aspergillus niger*) were studied.

© 2010 Published by Elsevier B.V.

1. Introduction

Many Schiff bases have received great attention due to their uses as chemical intermediate and perfume bases in dyes and rubber accelerators and in liquid crystals for electronic devices. Some Schiff bases were tested for fungicidal activity, which is related to their chemical structure [1]. A considerable number of articles have been published on the spectral behavior of Schiff bases and their application in different fields [2–7]. Recently, there has been a growing interest in new application using Schiff base and their transition metal complexes in the field of agriculture, medicine and in catalysis [8–13]. Although Schiff bases containing a heterocyclic nucleus have efficient biological activity, yet spectral studies of these compounds are comparatively minor [14,15].

In the present work, new Schiff base derivative and their complexes are prepared and investigated using the UV–vis, IR, ^1H NMR spectra and the biological activity also are studied.

2. Experimental

2.1. Materials and reagents

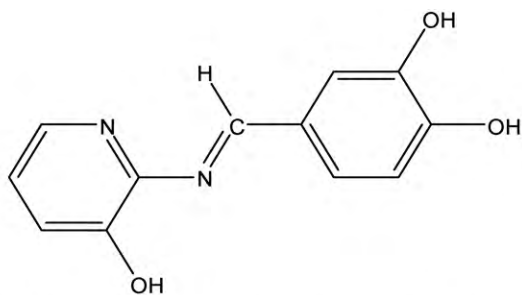
All chemicals used were of the analytical reagent grade (AR) and of highest purity available used without further purification.

2.2. Synthesis of Schiff base compounds (I–IV)

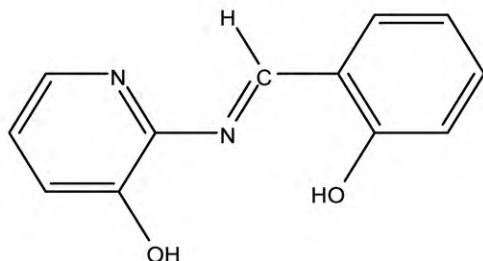
The Schiff base compounds were synthesized according to the recommended method for Schiff base compounds [16]. This was achieved by the following.

To a stirred and heated (60 °C) ethanolic solution of 2-amino-pyridin-3-ol (Aldrich) (110.11 g), solution of 5-bromo-2-hydroxy-benzaldehyde (Aldrich) (201.02 g), 3,4-dihydroxybenzaldehyde (Merck) (138.12 g), 4-dimethylaminobenzaldehyde (Merck) (149.19 g) and 2-hydroxybenzaldehyde (Aldrich) (122.12 g) in ethyl alcohol were added immediately in 1:1 mole ratio. The reaction mixture was heated at reflux on a water-bath for 4 h. By time the color of reaction mixture was changed to obtain the Schiff base compounds. The volume of the reaction mixture was evaporated to 30 ml and after cooling, the resulting Schiff bases were filtered off, washed with ethanol 70% and crystallized from the proper solvent. The purity and chemical structures were detected by sharp melting point, the elemental analysis (C, H, N), IR and ^1H NMR spectra (Table 1). The Schiff base derivative under study are shown as the following scheme:

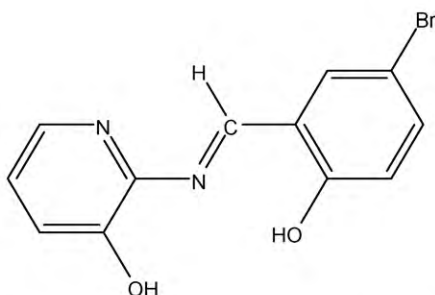
* Corresponding author. Tel.: +20 130122408034; fax: +20 133222875.
E-mail address: isahmed61@gmail.com (I.S. Ahmed).



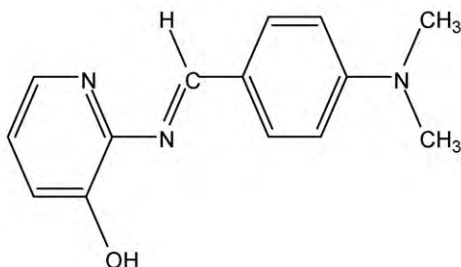
2-(1,2-Dihydroxybenzylidiaminomethyl) pyridine-3-diol (I)



2-(2-Hydroxybenzylideneamino)pyridine-3-ol (II)



2-(5-Bromo-2-hydroxybenzylideneamino)pyridine-3-ol (III)



2-[(4-Dimethylamino-benzylidene)-amino]-pyridin-3-ol (IV)

2.3. Synthesis of metal complexes

The solid chelates of stoichiometric ratios (1:1) (M:L) for some selected metal chelates were prepared by mixing the metal ions solutions with a hot alcoholic solution of ligands. The mixture was then refluxed on a water bath for about 8.0 h and then allowed to cool where by the solid chelates were separated and recrystallized from absolute ethanol, dried and persevered in a desiccator over dried silica gel.

2.4. Instruments and measurements

2.4.1. pH measurements

The pH value of all solutions was adjusted to the required value using pH-meter type HI 8014 HANA instruments.

2.4.2. Spectrophotometric measurements

All the absorption spectral measurements are made using Jasco V-530 (UV-vis) spectrophotometer (Japan) with scanning speed 400 nm/min, bandwidth 2.0 nm and equipped with 10.0 mm matched quartz cells. The transition energies of the visible absorption peaks are calculated [17] using Eq. (1):

$$E_j \text{ (kJ mol}^{-1}\text{)} = \frac{119.625}{\lambda_{(\text{nm})}} \quad (1)$$

2.4.3. Instruments

The IR spectra were recorded as KBr discs using Matson FT-IR spectrophotometer in the 4000–200 cm^{-1} range. The ^1H NMR spectrum of the ligands were performed using a varian EM 390–90 NMR spectrometer in $\text{d}^6\text{-DMSO}$ as solvent using tetramethylsilane (TME) as an internal standard. The microanalysis of C, H and N were performed in the Microanalytical Center of Cairo University.

2.5. Antibacterial and antifungal activities of the Schiff base compounds and their complexes

The well-plate method (diffusion methods) was followed with some modification [18]:

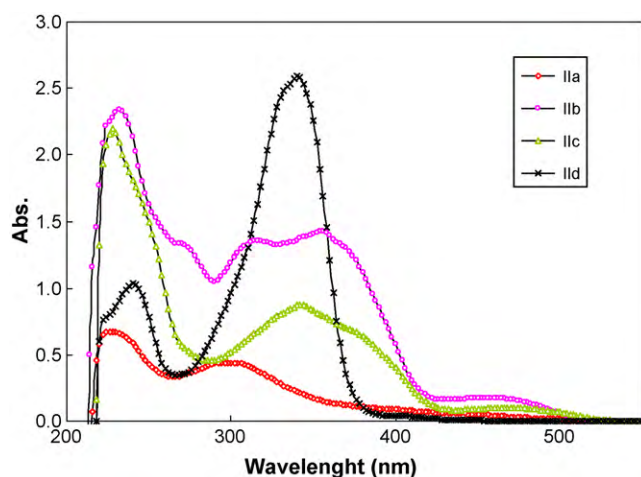
1. The spore suspension of the test organisms (Gram-negative bacteria, such as *Escherichia coli*, and *Agrobacterium* sp., and Gram-positive bacteria, *Staphylococcus aureus*, *Bacillus subtilis* and *Bacillus megatherium*), yeast (*Candida albicans*), and fungi (*Aspergillus niger*), was prepared in previously sterile and checked inoculating flasks, each contained 50 ml of previously and checked medium of the following composition for the target test organisms as following.

For bacteria, nutrient broth medium: (beef extract 3.0 g, peptone 10.0 g, H_2O 1000 ml). For yeast and fungi, Czapeks Dox broth medium: (sucrose 30.0 g, MgSO_4 0.5 g, KCl 0.5 g, FeSO_4 0.01 g, NaNO_3 3.0 g, K_2HPO_4 1.0 g, H_2O 1000 ml).

2. A solid medium containing the following ingredients for bacteria (g/l) (beef extract 3.0 g, peptone 10.0 g, agar 20.0 g, H_2O 1000 ml), and for yeast and fungi (sucrose 30.0 g, MgSO_4 0.5 g, KCl 0.5 g, FeSO_4 0.01 g, NaNO_3 3.0 g, K_2HPO_4 1.0 g, agar 20.0 g, H_2O 1000 ml), was sterilized and divided while warm (50:55 °C) in 15 ml portions among sterile Petri-dishes of 9 cm diameters.
3. 0.2 ml of the spore suspension was surface placed on the surface of the solid medium in the Petri dished and spread all over the surface.
4. 0.1 g of the test substances was weighted.
5. In Petri dishes containing the culture of one of the chosen microorganisms, one well of 10 mm diameter was made in the center of the dish. It was marked on the bottom of the dish, and filled with the 0.10 g of the test substances.
6. The Petri dishes were incubated at 5 °C for 2 h to permit good diffusion and then transferred to an incubator at 37 °C for 48 h for bacterial test organisms, and at 30 °C for 72 h for yeast and fungi test organisms.
7. Antimicrobial activities were observed after 48 h of incubation time for bacteria at 37 °C, and after 72 h of incubation time for yeast and fungi at 30 °C.

Table 1
Physical data of prepared ligands (I–IV).

Compd.	Empirical formula (F. Wt.)	Microanalysis, calc. (found)			M.P (°C)	Yield (%)	Color
		% C	% H	% N			
I	C ₁₂ H ₁₀ N ₂ O ₃ (230.22)	62.60 (62.90)	4.38 (4.23)	12.17 (12.03)	280	85	Gray
II	C ₁₂ H ₁₀ N ₂ O ₂ (214.22)	67.28 (65.14)	4.71 (4.81)	13.08 (11.99)	155	88	Yellow
III	C ₁₂ H ₉ BrN ₂ O ₂ (293.12)	49.17 (45.90)	3.09 (2.88)	9.56 (5.14)	173	73	Orange
IV	C ₁₄ H ₁₅ N ₃ O (241.29)	69.69 (68.40)	3.27 (7.31)	17.41 (12.03)	186	70	Blue

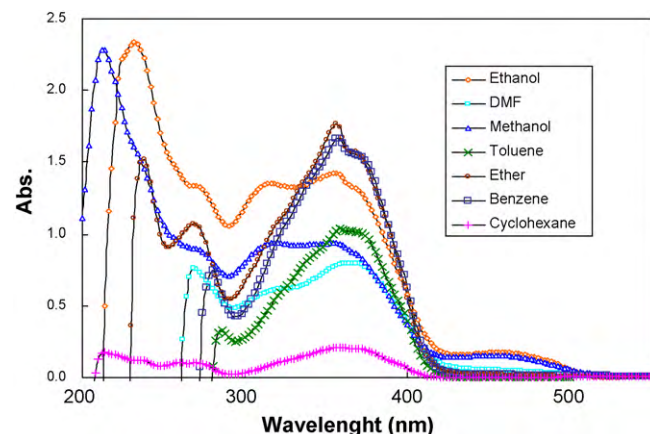
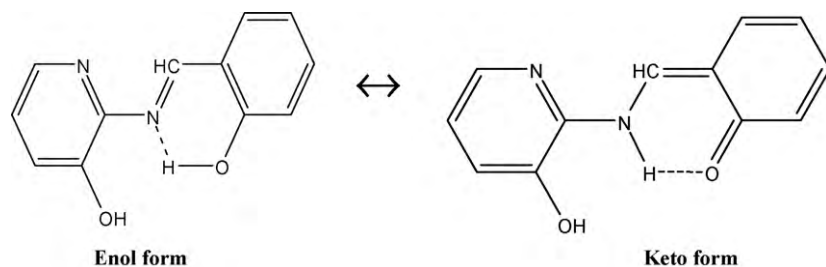
Fig. 1. Absorption spectra of (1×10^{-4} M) ligands I–IV in ethanol.

3. Results and discussion

3.1. The electronic absorption spectra

3.1.1. The electronic absorption spectra of the Schiff bases in ethanol

The electronic absorption spectra of Schiff base compounds (I–V) in ethanol display bands as shown in Fig. 1 and Table 2. The first two bands A and B are observed at range (225–240 nm) and (272–299 nm) are referred to the π – π^* transitions of the aromatic moieties with ϵ_{max} 0.67×10^4 and 2.33×10^4 L mol⁻¹ cm⁻¹ for I and II respectively. The donor substitute (hydroxyl group) causes a red shift for the pyridine moieties π – π^* band. The third band (C) ranged (314–343 nm) is due to π – π^* transition in the azomethine system (–CH=N–). This band is blue shift in ligands I and IV relative to ligand II. This can be explained by the inductive effect of the two methyl groups which increases the possibility for the blocking of electron density in CH=N group with ethanol molecules. For ligand II there is a shoulder at 272 nm which may be due to the delocalization of hydrogen atom from (OH) groups to give keto enol form which be represented as follows (Fig. 2):

Fig. 2. Absorption spectra of (1×10^{-4} M) ligand II in different organic solvents.

The longer wavelength band (D) at (400–469 nm) can be assigned to an intramolecular charge transfer interaction from aromatic group to the azo-methene group (–CH=N–) at 450, 460, 469 and 400 nm for ligands I, II, III and IV respectively which originate from the substituents phenyl ring which increases the dipole moment of the solute during the electronic transition, the Franck–Condon excited state is formed in a strained solvent cage of the oriented dipoles, thus the energy of the ground state is increased and this produces a bathochromic shift [19]. However, the hydrogen bond formation between the C=N group and the *o*-OH groups on the phenyl-ring shifts the charge transfer band to longer wavelength.

3.1.2. The solvatochromaticity of Schiff base derivatives in different organic solvent

The electronic absorption spectra of the investigated Schiff base ligands are collected in Table 3. For the spectra of Schiff base compounds. The spectrum of each compound exhibits mainly four bands. The lowest transition at (355–469 nm) and is assigned to the intramolecular charge transfer. This band shows positive solvatochromism (bathochromic shift) upon increasing the solvent polarity (Table 4). This means that a pronounced change in position of an electronic absorption band is accompanying a change in

Table 2
UV–vis spectra data of ligands (I–IV) in ethanol.

Comp.	Spectra bands							
	A		B		C		D	
	λ_{\max} (nm)	$\epsilon_{\max} \times 10^4$	λ_{\max} (nm)	$\epsilon_{\max} \times 10^4$	λ_{\max} (nm)	$\epsilon_{\max} \times 10^4$	λ_{\max} (nm)	$\epsilon_{\max} \times 10^4$
I	225	0.67	299	0.44	–	–	450	0.12
II	232	2.33	272	1.34	314	1.35	366	1.42
III	228	2.2	–	–	343	0.87	469	0.11
IV	240	1.03	–	–	340	2.59	400	0.11

the polarity of the medium. This observed behaviour is accounted as those molecules in the ground state and in the excited state indicate different polarities. This interpretation involves that highly simplifying assumption that Schiff bases with non-polarized ground state are more strongly polarized in protic solvents, because the high-energy polar structure of the excited state is stabilized. The energy difference between ground states and excited states is decreased and the excitation energy is decreased. The approximation of the energy levels expresses itself in a bathochromic shift of the spectrum with increasing polarity of solvents. The other absorption bands corresponding to the highest energy centered at (204–287 nm) are localized in the aromatic rings and are due to a ($\pi-\pi^*$) transition. These bands show a negative solvatochromism in solvent like diethyl ether, benzene and toluene. Those aprotic solvents destabilize the polarized electronic state. This leads to a hypsochromic shifting of the spectrum with decreasing solvent polarity. The UV–vis spectrum of Schiff base compounds II and III exhibit mainly two absorption bands. A positive solvatochromism is observed for ($n-\pi^*$) absorption in case of II whereas a negative solvatochromism is observed for this band in case of III where there is a bromide atom. The hypsochromic shift in the band follow the order $\text{Br} \gg \text{H}$ in an agreement with the order of their electronegativities.

Table 3
UV–vis spectra data of ligands (I–IV) in organic solvents.

Solvents	A		B		C		D	
	λ_{\max} (nm)	$\epsilon_{\max} \times 10^4$	λ_{\max} (nm)	$\epsilon_{\max} \times 10^4$	λ_{\max} (nm)	$\epsilon_{\max} \times 10^4$	λ_{\max} (nm)	$\epsilon_{\max} \times 10^4$
Ligand I								
DMF	–	–	291	1.16	–	–	466	0.21
Methanol	236	1.31	320	1.05	–	–	–	–
Toluene	–	–	295	0.06	370	0.05	–	–
Diethylether	240	0.11	–	–	332	0.08	–	–
Benzene	–	–	–	–	317	0.12	–	–
Cyclohexane	–	–	–	–	307	0.11	–	–
Ligand II								
DMF	–	–	269	0.79	321	0.617	355	0.77
Methanol	213	2.29	273	0.88	318	0.94	358	0.94
Toluene	–	–	285	0.33	–	–	369	1.03
Diethylether	238	1.52	269	1.06	356	1.77	372	1.57
Benzene	–	–	280	0.75	357	1.67	357	1.53
Cyclohexane	213	0.17	260	0.10	–	–	–	0.21
Ligand III								
DMF	–	–	268	0.95	344	1.21	374	1.13
Methanol	222	2.52	–	–	342	0.77	462	0.12
Toluene	–	–	288	0.23	343	0.84	–	–
Diethylether	237	1.06	–	–	342	0.55	372	0.51
Benzene	–	–	281	0.52	344	1.50	–	–
Cyclohexane	226	1.99	251	0.86	344	0.50	–	–
Ligand IV								
DMF	268	0.31	–	–	330	2.78	342	2.75
Methanol	207	0.49	240	0.51	343	1.96	–	–
Toluene	–	–	280	0.29	330	1.36	–	–
Diethylether	239	0.714	–	–	320	2.34	–	–
Benzene	–	–	–	–	330	1.18	–	–
Cyclohexane	211	0.622	234	1.09	312	2.33	–	–

The UV–vis spectra of ligands II and III in toluene exhibit two absorption bands, A band is formed at about 285 and 288 nm are assigned to a ($\pi-\pi^*$) transition which are blue shifted in all other solvents. Also, the second band at 358 and 345 nm for II and III respectively are blue shifted in the other solvents. A negative solvatochromism is noticed in all other solvents. The spectral shifts decrease with gradual introduction of the more polar solvent. In these solvents the hydroxyl groups in the pyridine moiety will be the proton acceptor center in the process of hydrogen bonds formation whereas the solvents that have the ability to form hydrogen bonds are the proton donors.

3.1.3. The electronic absorption spectra of the ligands in buffer solutions

The absorption spectra of 3×10^{-5} M of ligands I–V in universal buffer [20] solutions of varying pH in UV–vis region (200–600 nm) were done.

The spectra obtained indicate that the absorbance values and position of the absorbance bands change with pH of the medium due to the following:

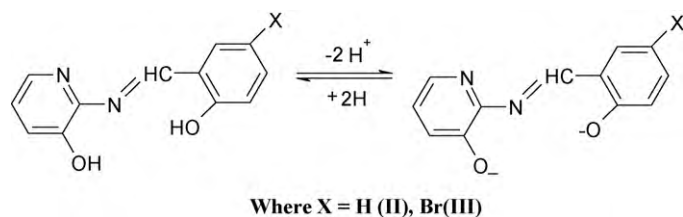
1. In case of ligand I, the absorption spectra shows an absorption band with $\lambda_{\max} = 230$ nm corresponding to unionized H_3L

Table 4
Prominent visible absorbance of ligands (I–IV) in different solvents and transition energy.

No.	Solvents	λ_{\max} (nm)	ϵ_{\max} (L mol ⁻¹ cm ⁻¹) × 10 ⁴	Transition energy (kJ mol ⁻¹)
Ligand I				
1	Ethanol	450	0.12	265.83
2	DMF	466	0.21	256.71
3	Methanol	320	1.05	373.83
4	Toluene	370	0.05	323.31
5	Diethylether	332	0.08	360.32
6	Benzene	317	0.12	377.37
7	Cyclohexane	307	0.11	323.11
Ligand II				
1	Ethanol	366	1.42	256.71
2	DMF	355	0.77	336.97
3	Methanol	358	0.94	334.15
4	Toluene	369	1.03	324.19
5	Diethylether	372	1.57	321.57
6	Benzene	357	1.53	335.08
7	Cyclohexane	365	0.21	327.74
Ligand III				
1	Ethanol	469	0.11	255.06
2	DMF	374	1.13	319.85
3	Methanol	462	0.12	258.93
4	Toluene	343	0.84	348.76
5	Diethylether	342	0.55	349.78
6	Benzene	344	1.50	347.74
7	Cyclohexane	344	0.50	347.74
Ligand IV				
1	Ethanol	400	0.11	299.06
2	DMF	342	2.75	349.78
3	Methanol	343	1.69	348.76
4	Toluene	330	1.36	362.50
5	Diethylether	320	2.34	373.83
6	Benzene	330	1.18	362.50
7	Cyclohexane	312	2.33	383.41

form, the extinction of this band decreases with increasing pH values of solution while another absorption band with $\lambda_{\max} = 310$ nm corresponding to the ionized H_2L^- form. The absorbance of this band decreases with increasing pH values of solution until pH 10.2. This behaviour indicates that at varying hydrogen ion concentration the equilibrium between undissociated and dissociated form are present in different ratios.

- The electronic spectra of ligands II and III show form different bands with two clear isosbestic points. These bands at $\lambda_{\max} = 225, 251, 310$ and 378 nm for ligand II and at $\lambda_{\max} = 220, 250, 313$ and 390 nm for ligand III. The first two band in both ligand decrease in absorbance with increase pH values of solution which indicate that these bands for undissociated form H_2L . The bands at higher wavelength increases in absorbance with increase pH values of solution and these bands corresponding to dissociated forms of two ligands. The isosbestic points at $\lambda_{\max} = 285$ and 347 nm for II and at $\lambda = 355$ and 278 nm for III indicating the existence of an acid base equilibrium between two different form of these compounds as shown in the following:



- The spectra of ligand IV show two different bands with λ_{\max} equals 244 and 352 nm corresponding to HL and L^- forms, respectively. The extinctions of the two bands increase with

increasing pH of the solution due to the change from the unionized form to the ionized form.

The pH-absorbance curves of the ligands at different wavelength corresponding to λ_{\max} are of typical Z or S shaped. This behaviour is utilized for the determination of the acid dissociation constant (pK_a) of these compounds by applying the half-height method (HHM) [21], the modified limiting absorbance method (LAM) [22], the colleter method (CM) [23] and the modified isosbestic point method (IPM) [24] (Table 5).

The values of pK_a are used in calculating the free energy change (ΔG^*) of the ionization process at 298 K from the relationship.

$$\Delta G^* = -2.303RT \log K$$

The increase of ΔG^* leads to the thermodynamically favored.

3.2. Electronic absorption spectra of the chelates

Based on the fact that, electronic absorption spectra are very diagnostic of the stereochemistry of metal chelates, the electronic absorption spectra of the solid chelates prepared in the present work are measured as nujol mull and in solution using DMF as solvent within the range 200–900 nm. The spectra of the free ligands (I–IV) in DMF indicate that $\nu(\text{cm}^{-1})$ of CT band are 26,666, 25,641, 24,330 and 27,322 cm^{-1} for I, II, III and IV respectively whereas that taken in nujol mull are 27,777, 27,855, 2770 and 26,737 cm^{-1} respectively. The $\nu(\text{cm}^{-1})$ of the CT band of all metal chelates of these ligands displays a red or blue shift in nujol mull and DMF compared to that of the free ligands. This generally confirms that such ligands interact with the metal ion, and the metal ion environments are different leading to the formation of different geometrical types of complexes. The difference in $\bar{\nu}(\text{cm}^{-1})$ values of the bands in DMF than in nujol mull indicates that the crystal

Table 5
The values of pK_a (dissociation constant) for Schiff base ligands at 298 K.

Ligand		pK_a					λ_{max} (nm)	ΔG° (kJ mol ⁻¹)
		HHM	LAM	CM	IPM	Av.V		
I	pK_{a1}	3.72	4.05	–	–	3.89	310	22.19
	pK_{a2}	6.20	6.36	7.02	–	6.53	230	37.26
	pK_{a3}	8.64	8.61	–	–	8.63	310	49.24
II	pK_{a1}	4.10	5.21	6.11	4.53	4.98	251	28.42
	pK_{a2}	6.20	6.34	–	5.92	6.15	310	35.09
III	pK_{a1}	6.82	6.43	–	5.83	6.36	313	36.29
	pK_{a2}	7.28	6.97	6.35	6.71	6.82	250	38.91
IV	pK_{a1}	7.79	7.21	8.01	–	7.67	352	43.76

HHM: Half height method, LAM: modified limiting absorbance method, CM: Colleter method, IPM: modified isosbestic point method, Av.V: average value, ΔG° : free energy change.

Table 6
Some selected bands of diagnostic importance for the IR spectra of ligands (I–IV).

Ligand				Assignment	
	I	II	III		IV
3568 (w)	–	3318 (w)	3232 (w)	3439 (w)	ν (OH)
–	–	3056 (w)	3047 (w)	3049 (w)	ν (CH) asym (Ar)
–	–	2922 (w)	2921 (w)	2916 (m)	ν (CH) asym (CH ₃)
2730 (w)	–	–	2872 (w)	2819 (w)	ν (CH) sym (CH ₃)
11631 (w)	–	1617 (s)	1624 (s)	1603 (s)	ν C=O
1590 (s)	–	1572 (m)	1576 (m)	1547 (m)	ν C=N
–	–	–	–	1437 (w)	ν N–CH ₃
1308 (m)	–	1292 (s)	1308 (w)	1312 (w)	ν (C–N)
1388 (w)	–	1373 (w)	1371 (w)	1372 (w)	δ (OH)
–	–	–	–	1167 (s)	δ (CH ₃)
1055 (w)	–	1096 (w)	1071 (w)	1065 (m)	ν (C–OH)
–	–	1032 (w)	1010 (m)	–	ν (CH=N)

sym: Symmetric, asym: asymmetric, s: strong, m: medium, w: weak, b: broadened.

state of the complexes differ in the solid state than in solution, and some kind of bonding was formed between the chelate and DMF.

The nujol mull electronic absorption spectra of copper complexes with Schiff base ligands gave charge transfer bands at 26,041, 22,371, 25,773 and 23,640 cm⁻¹ for I–IV complexes, respectively, with copper ion. The visible d–d electronic spectral band at 13,550 and 20,661 cm⁻¹ for complexes of Cu²⁺-I and Cu²⁺-IV respectively. The nujol mull electronic absorption spectra of cadmium complexes with the ligands under investigation gave charge transfer bands at 23,201, 23,041, 25,773 and 26,109 cm⁻¹ for Cd²⁺ complexes with I–IV respectively. Also, the nujol mull electronic absorption spectra of mercury complexes with ligands under studies gave charge transfer bands at 24,213, 24,213, 27,700 and 27,624 cm⁻¹ for Hg²⁺ complexes with Schiff base ligands I–IV, respectively. On the other hand, the nujol mull electronic absorption spectra of silver complexes with

the Schiff base ligands showed charge transfer bands at 26,246, 25,974, 28,011 and 23,255 cm⁻¹ for I–IV respectively. Also the visible d–d electronic spectra bands at 19,960, 15,337, 18,726 and 17,331 cm⁻¹ for silver complexes with I–IV respectively. Finally, the nujol mull electronic absorption spectra of zinc complexes with the Schiff base ligands showed charge transfer bands at 25,445, 23,474, 21,645 and 24,096 cm⁻¹ for ligands I–IV, respectively.

3.3. The infrared spectra

The IR-spectra of chelates, in comparison with those of the free ligands display certain changes which give an idea about the type of bonds and their structure.

All compounds exhibit two weak intensity bands at 2916–2922 and 2819–2872 cm⁻¹ corresponding to asymmetric and symmetric stretching vibrations of the aromatic C–H groups: $\nu_{(C=N)}$ give

Table 7
Assignment and chemical shift (ppm) of different types of protons of ligands under investigation.

Ligand	Chemical shift				
	(ppm) of protons			(ppm) of aromatic rings	
	H(1)	H(2)	H(3)	I	II
I	8.21	7.42	6.83	6.37–6.405 6.44–6.57	6.83–6.868
II	10.27	13.81	9.48	7.24–7.26 7.356–7.436	6.35–6.87 6.93–6.95
III	10.22	13.74	9.48	7.713–7.721	6.82–6.86 6.92–6.46
IV	9.67	3.05	7.68	6.82	6.77

medium intensity bands at 1547–1572 cm^{-1} . This band being shifted to lower wavenumber due to the contribution of the C=N in an intramolecular hydrogen bond. The spectra of these compounds exhibit the ν_{OH} as weak band at 3231–3439 cm^{-1} . While $\nu_{\text{C-OH}}$ bands are observed as weak intensity at 1065–1096 cm^{-1} . The low values of ν_{OH} reflects the existence of intramolecular hydrogen bond between OH and C=N groups [25]. The existence of coordinated water or water of hydration in all chelates cause difficulty in drawing conclusions from ν_{OH} band for the hydroxyl group. The participation of the hydroxyl group in chelation is confirmed by the appearance of new band at 420–540 cm^{-1} which is due to $\nu_{\text{(M-O)}}$ vibration. The bands at 370–400 cm^{-1} is attributed to $\nu_{\text{(M-N)}}$, while the bands appear at the range 340–350 cm^{-1} corresponding to $\nu_{\text{(M-Cl)}}$. The infrared spectra of the free Schiff base compounds under investigation exhibited medium intensity bands within 1292–1312 cm^{-1} are assigned to $\nu_{\text{C-N}}$ (Table 6).

3.4. ^1H NMR spectra of the ligands (I–IV)

The ^1H NMR spectra of schiff base compounds I–V are done and chemical shifts of the different signals are record in Table 7. The signals lying at very downfield side 8.21–10.27 ppm are due to the hydrogen of OH group attached to the pyridine ring, while signals lying in range 7.42–13.81 ppm are referred to the OH group attached to phenyl ring. A new multiple signals at range 6.37–7.713 ppm are due to the protons of the phenyl group.

Also, in ligand IV the signal at 3.05 ppm is due to the two methyl groups attached to the nitrogen atom. The signals lying in range 6.83–9.48 ppm are referred to the proton of azomethine group of these Schiff base compounds. The signals of OH group lying at downfield side 7.42 ppm for ligand can be attributed to the contribution of the OH group in intramolecular and intermolecular hydrogen bond as following:

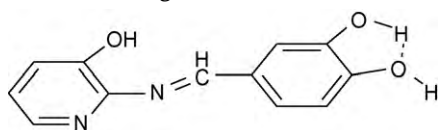


Table 8

Responses of various microorganisms to the Schiff bases and their complexes in vitro culture (numbers in the table represent the extent of the inhibition zone diameters in mm).

Compound	<i>Escherichia coli</i> 0.1 g	<i>Bacillus subtilus</i> 0.1 g	<i>Candida albicans</i> 0.1 g	<i>Aspergillus niger</i> 0.1 g	<i>Staphylococcus aureus</i> 0.1 g	<i>Agrobacterium sp.</i> 0.1 g	<i>Bacillus megatherium</i> 0.1 g
I	25	0	0	0	0	0	0
Cu ²⁺ -I	20	25	30	0	15	0	0
Cd ²⁺ -I	30	25	10	0	20	0	20
Hg ²⁺ -I	40	30	20	0	20	0	15
Ag ⁺ -I	50	35	30	0	25	0	15
Zn ²⁺ -I	25	20	0	0	0	0	0
II	20	20	22	0	20	25	19
Cu ²⁺ -II	20	25	15	0	10	15	10
Cd ²⁺ -II	15	20	10	0	0	0	0
Hg ²⁺ -II	20	20	25	0	10	0	15
Ag ⁺ -II	30	20	15	0	15	10	10
Zn ²⁺ -II	0	0	0	0	0	0	0
III	35	30	30	0	40	35	30
Cu ²⁺ -III	10	10	0	0	0	0	0
Cd ²⁺ -III	15	20	10	0	15	10	0
Hg ²⁺ -III	0	0	0	0	0	0	0
Ag ⁺ -III	0	0	0	0	0	0	0
Zn ²⁺ -III	0	0	0	0	0	0	0
IV	30	25	20	0	25	30	35
Cu ²⁺ -IV	20	10	15	15	20	20	15
Cd ²⁺ -IV	15	20	20	10	10	10	15
Hg ²⁺ -IV	30	25	10	25	15	15	10
Ag ⁺ -IV	25	20	20	0	10	0	20
Zn ²⁺ -IV	0	0	25	0	0	0	0



Fig. 3. Biological activity on some prepared metal complexes.

3.5. Biological activity studies

In this study (Fig. 3), microorganisms representing different microbial categories (two Gram-negative bacteria, *E. coli* and *Agrobacterium sp.*), three Gram-positive bacteria (*S. aureus*, *B. subtilus* and *B. megatherium*), yeast (*C. albicans*), and fungi (*A. niger*), were used. The study included 18 compounds, 3 ligands (I, II and III) and 15 complexes of different metal ions (Cu²⁺, Cd²⁺, Hg²⁺, Ag⁺ and Zn²⁺). The diffusion agar technique was used to evaluate the antibacterial activity of the ligands and the chelates [18].

The results of the bacterial screening of the synthesized compounds are recorded in Table 8. As about ligand I and III the data reflect that these two Schiff base ligands have an activity in comparison with I, whereas their complexes have moderate activity with different degrees except in case of Zn²⁺ complex in case of I, II and III, and Hg²⁺ and Ag⁺ complexes in case of III.

Against all the organisms, ligand I did not exhibit any remarkable activity compared with its complexes whereas all complexes showed moderate to high activities. It is suggested that the

complexes having antimicrobial activity may act either by killing the microbe or by inhibiting multiplication of the microbe by blocking their active sites [26].

Such increased activity of the metal chelates can be explained on the basis of chelation theory. On chelation, the polarity of the metal ion will be reduced to a great extent due to the overlap with the ligand orbital. Further, it increases the delocalization of π -electrons over the whole chelate ring and enhances the lipophilicity of the complexes [27].

4. Conclusions

Schiff base compounds (I–IV) and their chelates are prepared and characterized by using elemental analysis (C, H, N), IR, ^1H NMR and UV–vis spectra. The electronic absorption spectra of the ligands are recorded in different solvents and in universal buffer solutions. The pK_a of the compounds I–IV are determined applying different methods. The biological activity against bacterial species and fungi are investigated successfully.

References

- [1] A.S.M. AL-Srihri, H.M. Abdel-Fattah, J. Therm. Anal. Calorim. 71 (2003) 643.
- [2] S.A. Serron, C.M. Haar, S.P. Noan, Organometallics 16 (1997) 5120.
- [3] A.F. Marinovich, R.S. O'Mahony, J.M. Waters, T.N.M. Waters, CROATICA Chem. Acta 72 (1999) 685.
- [4] W.T. Gao, Z. Zheng, Molecules 7 (2002) 511.
- [5] J. Vanco, O. Svajlenova, E. Racnska, J. Muselik, J. Valentova, J. Trace Elem. Med. Biol. 18 (2004) 155.
- [6] T. Ueno, M. Ohashi, M. Kono, K. Kono, A. Suzur, T. Yamane, Y. Watanabe, Inorg. Chem. 43 (2004) 2852.
- [7] A.A. Khandar, K. Nejati, Z. Rezvani, Molecules 10 (2005) 302.
- [8] B.S. Holla, M. Mahalinga, M.S. Karthikeyan, B. Poojary, P.M. Akberali, N.S. Kumari, Eur. J. Med. Chem. 40 (2005) 1173.
- [9] I. Kaya, S. Cullhaglu, M. Gull, Synth. Met. 156 (2006) 1123.
- [10] Z. Guo, R. Xing, S. Liv, Z. Zhong, X. Ji, L. Wang, P. Li, Carbohydr. Res. 342 (2007) 1329.
- [11] L. Shi, H.M. Ge, S.H. Tan, H.Q. Li, Y.C. Song, H.L. Zhu, R.X. Ten, Eur. J. Med. Chem. 42 (2007) 1329.
- [12] V.P. Daniel, B. Murukan, B.S. Kumori, K. Mohanan, Spectrochim. Acta Part A (2008).
- [13] K.K. Upedhay, A. Kumar, S. Upadhyay, P.C. Mishra, J. Mol. Struct. 873 (2008) 5.
- [14] K. Kurzak, I.K. Biernacka, B. Zurowska, J. Solut. Chem. 28 (2) (1999).
- [15] S.M. Ben-Saber, A.A. Maihub, S.S. Hudere, M.M. El-ajaily, Microchem. J. 81 (2005) 191.
- [16] E. Tas, I. VCar, V.T. Kasumov, A. Kilic, A. Bulut, Spectrochim. Acta Part A 68 (2007) 463.
- [17] G. Laus, H. Schottenberger, N. Schuler, K. Wurst, R.H. Herber, J. Chem. Soc. Perkin Trans. 2 (2002) 1445.
- [18] N.S. Egorov, Microbe-antagonists and Biological Assessment of their Antibiotics Activity, Vysshaya Shkola Publishers, Moscow, Russia, 1965.
- [19] C. Reichardt, Solvent and Solvent Effects in Organic Chemistry, 3rd ed., Wiley VCH, Germany, 2004.
- [20] H.T.S. Britton, Hydrogen Ions, 4th ed., Champan and Hall, 1952, p. 364.
- [21] R.M. Issa, J. Chem. U.A.R. (Egypt. J. Chem.), 14 (1971) 133.
- [22] R.M. Issa, A.H. Zewail, J. Chem. U.A.R. (Egypt. J. Chem.), 14 (1971) 461.
- [23] J.C. Colleter, Ann. Chim. 5 (1969) 415.
- [24] I.M. Issa, R.M. Issa, M.R. Mahmoud, Y.M. Temenk, Z. Phys. Chem., Leipzig, 233 (1973) 289.
- [25] H.H. Abdel-Kader, R.M. Issa, M.M. Abousekkin, S.S. Assar, Delta J. Sci. 11 (1987) 171.
- [26] G.G. Mohamed, Spectrochim. Acta Part A 64 (2006) 188.
- [27] K.Y. El-Baradie, Monatshefte für Chem. 136 (2005) 1139.